



Contents lists available at ScienceDirect

## Medical Engineering and Physics

journal homepage: [www.elsevier.com/locate/medengphy](http://www.elsevier.com/locate/medengphy)

## Assistive locomotion device with haptic feedback for guiding visually impaired people

Mario F. Jiménez<sup>a,\*</sup>, Ricardo C. Mello<sup>b</sup>, Teodiano Bastos<sup>b</sup>, Anselmo Frizera<sup>b</sup><sup>a</sup> Department of Bioengineering, Faculty of Engineering, Universidad El Bosque, Bogotá D.C., Colombia<sup>b</sup> Postgraduate Program in Electrical Engineering, Federal University of Espírito Santo, 29075-910 Vitória, Brazil

## ARTICLE INFO

## Article history:

Received 10 December 2018

Revised 16 March 2020

Accepted 5 April 2020

Available online xxx

## Keywords:

Admittance control

Visual impairment

Haptic feedback

Smart walker

## ABSTRACT

Robotic assistive devices are able to enhance physical stability and balance. Smart walkers, in particular, are also capable of offering cognitive support for individuals whom conventional walkers are unsuitable. However, visually impaired individuals often need additional sensorial assistance from those devices. This work proposes a smart walker with an admittance controller for guiding visually impaired individuals along a desired path. The controller uses as inputs the physical interaction between the user and the walker to provide haptic feedback hinting the path to be followed. Such controller is validated in a set of experiments with healthy individuals. At first, users were blindfolded during navigation to assess the capacity of the smart walker in providing guidance without visual input. Then, the blindfold is removed and the focus is on evaluating the human-robot interaction when the user had visual information during navigation. The results indicate that the admittance controller design and the design of the guidance path were factors impacting on the level of comfort reported by users. In addition, when the user was blindfolded, the linear velocity assumed lower values than when did not wear it, from a mean value of 0.19 m/s to 0.21 m/s.

© 2020 IPEM. Published by Elsevier Ltd. All rights reserved.

## 1. Introduction

According to the estimates of the World Health Organization, 285 million people present some visual impairment and 14 percent of them are blind [1]. Additionally, 82 percent of the blind population is aged over 50 years old [1]. Such situation is also of concern, considering that the number of elderly people is projected to reach nearly 2.1 billion in 2050 [2].

Mobility and vision are two of the human faculties that can be largely affected by age [3]. Gait disorders can often be linked to causes such as poor vision, frontal gait disorder associated with vascular encephalopathy, and osteoarthritis of the hips or knees [3]. Cardiopulmonary and musculoskeletal disease are conditions that can slow down gait speed while also inflicting losses in vision, standing balance, and overall physical activity [4]. Stroke is another example of an event that can also lead to vision and locomotion reduction [4,5]. Elderly with vision and gait impairments may appear confused, especially when navigating in an unknown facility [5].

In general, visually impaired individuals can use technical aids such as canes and guide dogs [6]. However, those solutions may not be suitable to individuals that also present gait impairments [7]. In such cases, typical navigation aids can only offer limited physical assistance [7]. Despite enhancing partial body weight support, improving balance, and independence during locomotion, mobility assistive devices usually provide little or no sensorial assistance or environmental information to its users [8].

The incorporation of robotics into conventional walkers enhances support for individuals with gait disabilities. Smart Walkers (SW) are robotic devices capable not only of providing physical support, sensorial and cognitive assistance, but also health monitoring through the use of advanced human-machine interaction [9]. Taking advantage of the physical assistance provided by the SWs, sensorial information may be used to provide cognitive assistance and guide people with both mobility and vision impairments. In addition, when providing guidance, environmental information must be considered within the interaction loop. Therefore, the *Human-Robot Interaction* (HRI) should take into account environmental cues to provide proper interaction with the user, thus generating the *Human-Robot-Environment Interaction* (HREI) [10].

The use of HREI to guide blind individuals has explored an extended range of sensors and interfaces. One of the most prominently used sensor is the force sensor, often found in Smart

\* Corresponding author.

E-mail addresses: [mjimenezh@unbosque.edu.co](mailto:mjimenezh@unbosque.edu.co), [mariof.jimenez@gmail.com](mailto:mariof.jimenez@gmail.com) (M.F. Jiménez), [ricardo.mello@ieee.org](mailto:ricardo.mello@ieee.org) (R.C. Mello), [teodiano.bastos@ufes.br](mailto:teodiano.bastos@ufes.br) (T. Bastos), [anselmo@ele.ufes.br](mailto:anselmo@ele.ufes.br) (A. Frizera).

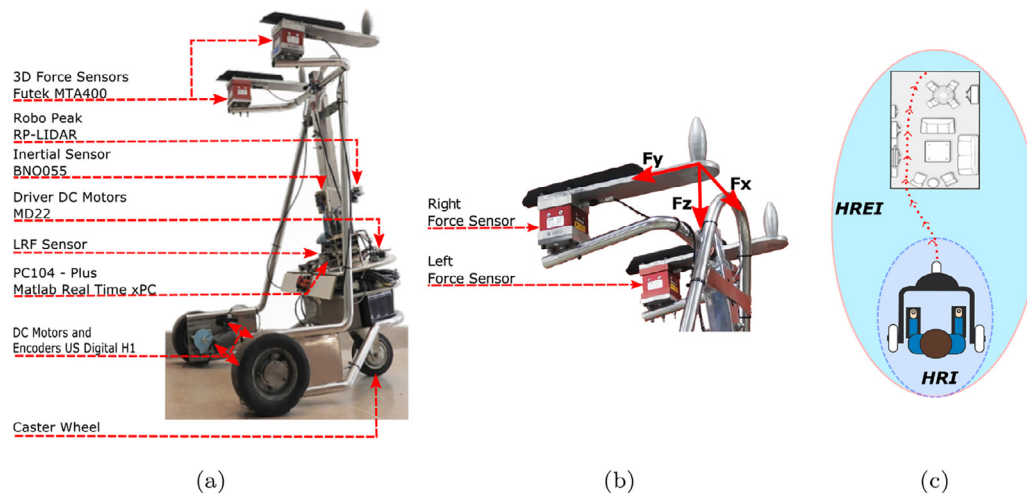


**Fig. 1.** a) Smart Walker of UFES/Brazil. b) Physical interaction system based on force sensors. c) Interaction layers.

**Table 1**  
Table of abbreviations.

| Abbreviation | Definition                                 |
|--------------|--|
| DOF          | Degrees of Freedom                         |
| FLC          | Fourier Linear Combiner                    |
| HREI         | Human-Robot-Environment Interaction        |
| HRI          | Human-Robot Interaction                    |
| LRF          | Laser Range Finder                         |
| MWW          | Mann-Whitney-Wilcoxon                      |
| SC           | Smart Cane                                 |
| SLAM         | Simultaneous Localization and Mapping      |
| SW           | Smart Walker                               |
| WFLC         | Weighted-Frequency Fourier Linear Combiner |

Canes (SC) to detect the user's motion intention [11]. Ultrasonic [11,12] and laser-based [7,13] sensors are also employed to detect obstacles and to provide navigational information. Wearable sensors and vibration motors have been used together with SCs and SWs as interfaces to assist navigation of blind individuals [7,14]. Nevertheless, such interfaces might be considered to be unnatural or uncomfortable. Moreover, the use of such interfaces demands from the user cognitive interpretation of signals, which may be confusing and induce fatigue [15].

Passive SWs (i.e., those without wheel actuators) have been used to assist the navigation of blind individuals [7]. Nevertheless, active SWs (i.e., those that uses actuators to add energy into the system) can offer full assistance in navigation and guidance [16] and little literature has been reported on guidance of visually impaired people. In addition, HREI concepts in such application should be discussed with more attention, as well as the user experience which provide quantitative impressions of the SW performance. Furthermore, HREI strategies should be natural and intuitive for the user in order to provide a good usability and user experience [10], allowing the continued control on the SW (Table 1).

In this work, we implement an admittance controller in an SW to guide visually impaired individuals throughout the environment. By means of haptic feedback, the control strategy guides the user locomotion through a desired path. Force sensors located under the forearm supports are used to detect the user's motion intention. Thus, the user is able to perform not only a comfortable gait speed with the SW, but also can control the start and end of the locomotion. The SW's linear velocity controller is directly dependant on the interactions forces, and a function of a virtual torque is used for the angular velocity control. Angular velocity depends on the angular position error of the SW in relation to the desired path.

The proposed controller is based on cognitive and physical interaction, relying on haptic feedback and physical contact between the user and the SW, respectively. Such interaction is used to inform the desired path to the user.

As the user needs to keep on the path for a safe navigation, inputs related with independent intention to turn do not influence in the guidance, thus, the tracking error is lower. In addition, this work also focused on to identify interaction parameters such as the restraints on SW velocities and design of the desired path, as these can affect the user experience with the SW during navigation.

## 2. Related work

Many research groups have worked over the last few decades on health-care with focus on assisting mobility and visually impaired people [7,12,17]. As smart canes might not offer proper weight support or assistance for those with moderate severe gait disorders [18], most of the related work deals with SWs [7,18].

The PAM-AID [19] aimed to provide guidance to visually impaired elderly individuals by gathering the user's motion intention to lead the way through corridors while warning about surrounding obstacles. Guido [20], an evolution of the PAM-AID, could provide point-to-point guidance by generating a path based on a simultaneous localization and mapping (SLAM) feature. On a more recent work, Wachaja et al. [7] presented a solution to navigate visually impaired individuals using an off-the-shelf rollator modified with laser sensors. Such SW relies on two different vibro-tactile interfaces to provide navigational information and presented two operation modes: one in which the user was only informed about surrounding obstacles, and another one in which the user was guided to a specific location. This point-to-point guidance leveraged mapping features to conduct the user throughout a path, avoiding both static and dynamic obstacles. Experiments revealed that users preferred the haptic interface on the handles over the belt, which was considered a rather obtrusive interface.

Interaction methods that rely on haptic interfaces are more commonly employed when guiding the user. As an example, Lu et al. [21] introduced an active SW that compared the user's force inputs against the desired path in order to guide while maintaining some degree of freedom for deviations. Werner et al. [16] states that full motion control provides maximum assistance in navigation and guidance, thus pointing to the use of active SWs. Nevertheless, the SW platform should not only offer physical, sensorial and cognitive assistance, but also offer a natural and intuitive way of navigate through the environment.

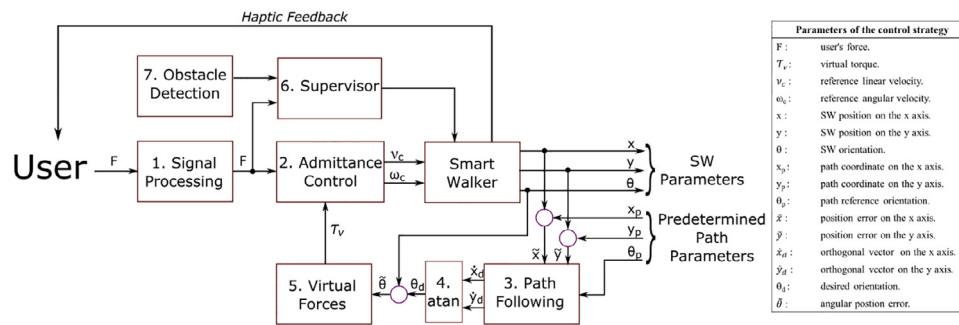


**Fig. 2.** Block diagram of the controller strategy to guide visually impaired people.

### 3. Materials and methods

The UFES Smart Walker (see Fig. 1) is the robotic platform used in this work. It consists of a metal frame, a pair of differential rear wheels driven by DC motors, and a front caster wheel. An embedded computer PC/104-Plus standard is integrated into a real-time architecture based on Matlab-Simulink Real-Time xPC Target Toolbox.

Figure 1c illustrates the interaction layers between human, walker, and environment. Within the UFES SW platform, the HRI strategy is performed relying on both physical and cognitive interaction, based on two kinds of sensors: a pair of 3D force sensors MTA400 (Futek, US), installed under the forearm supporting platforms (see Fig. 1b) to detect the user's motion intentions, and a laser range finder (LRF) sensor URG-04LX (Hokuyo, Japan) to obtain the distance between the user's legs and the walker [22].

HREI is based on environmental information and the robot's position, which is determined by the odometry. Odometry estimation is performed by filtering data from optical encoders H1 (US Digital, US) and from a 9 DOF inertial sensor BNO055 (Bosch, Germany). A second LRF sensor, a RP-LIDAR (Robo Peak, China), is placed in the front of the SW for obstacle detection.

### 3.1. Guidance control strategy

The block diagram of control strategy adopted in this work is shown in Figure 2. It is based on the controller presented by the authors in a previous work [10], which guides the user across a pre-established path. The path follower controller proposed by Andaluz et al. [23] is used to provide the desired orientation of the SW. In order for the interaction to be perceived as natural while still not allowing the user to deviate from the path, the robot's linear velocity is directly linked to user's interaction forces, whereas the steering velocities depend also the desired orientation. In other words, the user cannot consciously changing the SW's orientation, which depends on the SW's relative position to the path. This is done to avoid deviations from the path.

The force sensors are responsible for capturing the user's intention of movement, and data from each sensor are translated into a forward force, henceforth referred to merely as the force (box 1 Fig. 2). The human force  $F_H$  and human torque  $\tau_H$  are obtained from the y axis signals of each force sensor (see Fig. 1b), as shown in Eqs. (1) and (2).

$$F_H(t) = -\frac{F_{L_Y}(t) + F_{R_Y}(t)}{2} \quad (1)$$

$$\tau_H(t) = -\frac{F_{L_Y}(t) - F_{R_Y}(t)}{2} \times d, \quad (2)$$

where  $F_{L_y}(t)$  is the force on the left arm,  $F_{R_y}(t)$  is the force on the right arm, and  $d$  is the distance between sensors [10].

To detect the user's motion intention, the method proposed by Cifuentes and Frizera [22] was used, in which a Fourier Linear Combiner (FLC) algorithm estimates and cancels the cadence component is used to estimate and cancel cadence component of each input signal ( $\hat{F}_{Ly}(t)$  and  $\hat{F}_{Ry}(t)$ ). A Weighted-Frequency Fourier Linear Combiner (WFLC) algorithm then filters the signals to remove gait-induced disturbances.

The admittance controller (box 2 Fig. 2) proposed by Jiménez et al. [10] was used to produce linear control velocities  $v_c(t)$  from the  $F_H(t)$  signal, as shown in Eq. (3).

$$v_c(t) = \frac{F_H(t) - m_v \dot{v}(t)}{d_v} \quad (3)$$

The mass  $m_v$  and damping  $d_v$  are used to define the HREI dynamics. As the user intention to turn does not affect the guidance, the human torque ( $\tau_H(t)$ ) is measured only for evaluating the cognitive interaction through the haptic feedback obtained by the user's physical contact with the SW. The angular control velocity  $\omega_c(t)$  (i.e., the angular velocity output from the admittance controller) is used to point and conduct the user into the desired path and further, maintain the user on the path.

A path following controller is used to guide the user across the desired path (box 3 Fig. 2). The closed loop equation gives the SW's reference – or desired – orientation (see Eq. (4)).

$$\begin{bmatrix} \dot{x}_d \\ \dot{y}_d \end{bmatrix} = \begin{bmatrix} v_r \cos \theta_p + l_x t \tanh\left(\frac{k_x}{l_x} \tilde{x}\right) \\ v_r \sin \theta_p + l_y t \tanh\left(\frac{k_y}{l_y} \tilde{y}\right) \end{bmatrix}, \quad (4)$$

where  $v_r$  is the path desired velocity;  $\theta_p$  is the path reference orientation, defined by the tangent of the nearest point to the path;  $l_x$  and  $l_y$  determine the saturation limits of the position error;  $k_x$  and  $k_y$  are constant gains that establish the linear zone of the position error; and  $\tilde{x}$  and  $\tilde{y}$  are the position errors of the SW with respect to the path [10]. Eq. (5) is used to estimate the reference or desired orientation  $\theta_d$  for the SW (box 4 Fig. 2), which is obtained from the orthogonal vectors  $\dot{x}_d$  and  $\dot{y}_d$ .

$$\theta_d = \text{atan}\left(\frac{\dot{y}_d}{\dot{x}_d}\right). \quad (5)$$

Once  $\theta_d$  is defined, it is possible to calculate the orientation error  $\tilde{\theta}$  between the reference orientation  $\theta_d$  and the SW orientation  $\theta$ , which is shown in Eq. (6).

$$\tilde{\theta} = \theta_d - \theta \quad (6)$$

The orientation error is the spatial information used to set the virtual forces (see Fig. 3a and 3 b), that are further used to define the virtual torque ( $\tau_v(t)$ ) (box 5 Fig. 2). Hence, the equations are

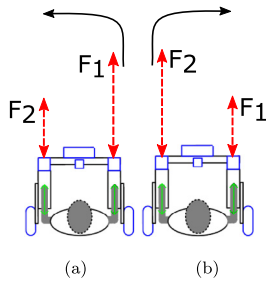


Fig. 3. Virtual force modulation. a) Left turn. b) Right turn.

represented by:

$$F_1(t) = k(1 + \tanh(\tilde{\theta})), \quad (7)$$

$$F_2(t) = k(1 - \tanh(\tilde{\theta})), \quad (8)$$

$$\tau_v(t) = \frac{F_1(t) - F_2(t)}{2} \cdot d, \quad (9)$$

where  $k$  is gain constant used for properly setting forces, and  $d$  is the distance between sensors.

Then, the virtual torque (see Eq. (9)) is used to calculate the angular control velocity  $\omega_c(t)$  (see Eq. (10)) of the admittance controller:

$$\omega_c(t) = \frac{\tau_v - m_\omega \dot{\omega}(t)}{d_\omega}, \quad (10)$$

In Eq. (10) the mass  $m_\omega$  and damping  $d_\omega$  also participate in the HREI dynamics.

The end-result of this control strategy is that the user is able to control the movement of the SW during the interaction, and the human turn intention which is not having into account for  $\omega_c(t)$ , may not be perceived as a restriction. When the user desires to steer in a way that would lead to path deviation, the haptic feedback indicates the correct path to the user, and, as result, the correct direction to follow is presented to the user.

A safety supervisor is in charge of determining if the user can start the locomotion and three safety factors are considered. The first one establishes a threshold  $\sigma_f$  in the  $z$  axis of each force sensor, which is used for the user's partial body weight support on the SW. If a threshold is not surpassed, no control velocities are sent to the motors. Once the threshold is surpassed in each sensor, the controller sends the  $v_c(t)$  and  $\omega_c(t)$  values to the drivers. In the second rule, a semicircle protection area with 70 cm of radius in front RP-LIDAR laser sensor is established to avoid collisions, thus, if the laser sensor detects an obstacle within the semicircle,  $v_c(t)$  and  $\omega_c(t)$  become zero. In addition, the linear velocity was limited to 0.25 m/s, as a third safety factor. Such safety factors were imple-

mented to guarantee the user's safety during navigation with the SW.

### 3.2. Controller simulation and path design

A SW is simulated in Matlab to verify the proposed controller's behavior on a given set of paths. The UFES SW kinematic model and an approximation of its dynamic model are used in the simulation. The admittance control strategy inserts inertia in the system by the mass  $m_v$  of the linear velocity equation (see Eq. (3)). When the robot must steer along the path, the linear velocity, the controller inertia, and the path attraction – induced by the path following controller – are combined to generate the steering movement. All those factors affect the user's stability and balance, as the maneuverability may decrease. In order to understand how this might impact on guidance and how it is related to the way the desired path is established, the simulations accounted for multiple path designs.

Figure 4 shows the simulation results for three different paths. The linear velocity of the simulated SW was limited to 0.58 m/s, as this is the typical gait speed for a usual pace in elderly without any gait disorder [24]. The forward force  $F_H$  was constant and established in 8 N. Such value results in maximum linear velocity. The other parameters of the guidance control strategy are defined in such a way that the robot could follow the desired path.

Figs. 4 a and 4 b show that the robot surpasses the desired path, due to the sharp shape of the curve and the inertia inherent to the controller. These results in intense additional angular movement to correct the orientation error and bring the robot back the desired path.

Figure 4 c presents a soft curve with radius of 1.4 m. Now, the robot follows the desired path and does not present any additional movement to keep on the path. Although the human factor is usually not considered for path generation in traditional robotics, soft curves along a path are natural to humans, and the absence of oscillatory movements may take an important role in the user experience during physical interaction with robots.

In that sense, both the maximum allowed linear velocity and the curve form directly affect the travel along the path. Thus, is necessary to limit the maximum value of linear velocity and the minimum value of the curve radius. Furthermore, the inertia added by the admittance controller plays a positive role on guidance when these limits are included.

### 3.3. Experimental validation

Preliminary experiments were conducted to validate the proposed control strategy and to evaluate its performance. Fifteen people (eight women) participated in the experiments; partici-

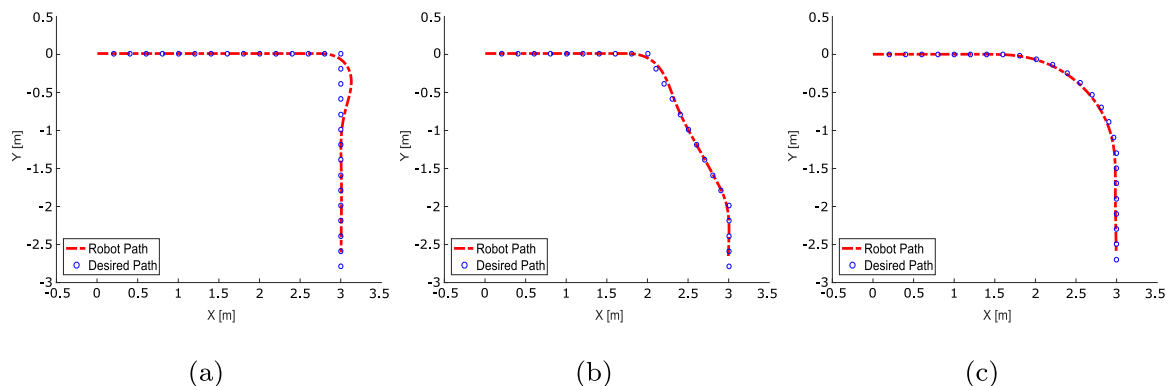


Fig. 4. Control strategy simulated for different path designs.





**Fig. 5.** Experiment scenario: the trial starts at the building entrance (box 1) and the participant is guided to a room (box 5).

pants had no previous training with the SW and presented no disabilities. The height of participants ranged from 1.53 m to 1.72 m, and the body mass ranged from 54 kg to 73 kg. Experiments are performed in a non-structured environment (see [fig. 5](#)); the designed path, composed by three straight line segments linked by soft curves, requires the user to go over different surfaces (i.e., rug and corridor floor) and also to pass nearby tables and other objects. Details regarding the tuning of the control parameters can be found at the online supplementary material.

Each participant performed a trial consisting of two parts: during the first part, the participant is unaware of the path and is required to use a blindfold see [Figure 5](#); during the second part of the experiment, the guidance was performed without the blindfold. In both experiments, the user was able to interact and transmit movement intentions to start or stop the locomotion, and also to regulate the desired speed. During the first part of the experiment, the HREI and the controller behavior are observed to assess the proper functioning of the guidance strategy when there is no visual feedback to the user. Thus, the user interacts with the environment through the SW, and the attention is on the guiding strategy. Later, during the second part, the focus is on the haptic

feedback and the user physical and cognitive interactions while maneuvering the SW. The presence of the visual feedback changes the perception of the user. Therefore, although the user already knows the general path, the exact path is still unknown. Thus, as the controller attempts to keep the user on path, the interaction is affected by the user's conscious intentions. The linear velocity was limited to 0.25 m/s in both parts of the experiment as a security factor. This limit in the linear velocity is enough to provide good and comfortable locomotion and guidance during the interaction with the UFES SW [\[10\]](#).

#### 4. Results and discussion

In the experiments, the participants interacted with the SW as expected. All experiments used the same initial pose and path. [Figure 6](#) shows odometry data from two participants, one of them performing the first part of the trial, wearing the blindfold ([Fig. 6a](#)), and the other one, the second part of the trial, without the blindfold ([Fig. 6b](#)). In both cases the controller was able to guide and maintain the user along the desired path. Due to the absence of sharp curves and the fact that the user always starts in a point inside the desired path, there were no path deviations, as expected.

[Figure 7](#) a shows a representative result observed when the subject is wearing the blindfold. The physical interaction forces between the user and the SW, and the control signals behavior are shown in the [Figure 7a](#). Once the SW starts the movement, a small force signal (around 0.2 N) is necessary to maintain the locomotion with the SW along the desired path. When wearing a blindfold, the controller haptically induces a torque on the user due to the physical interaction.

Thus, in the straight segments of the path, the torque signal  $\tau_H(t)$  is around zero. However, such torque can be clearly perceived during the curves, being particularly stronger in the second curve of the desired path. At the beginning of that curve, the torque  $\tau_H(t)$  detected is contrary to the curve direction (see red dotted line in second curve zone in [Fig. 7a](#)), as the user was not able to perceive the beginning of the curve and attempted to keep going straight ahead. Once the user interprets the haptic feedback, the user follows the interaction and applies torque in the same direction of the curve. This interaction was perceived as intuitive and the controller strategy is able to indicate to the user the path to follow.

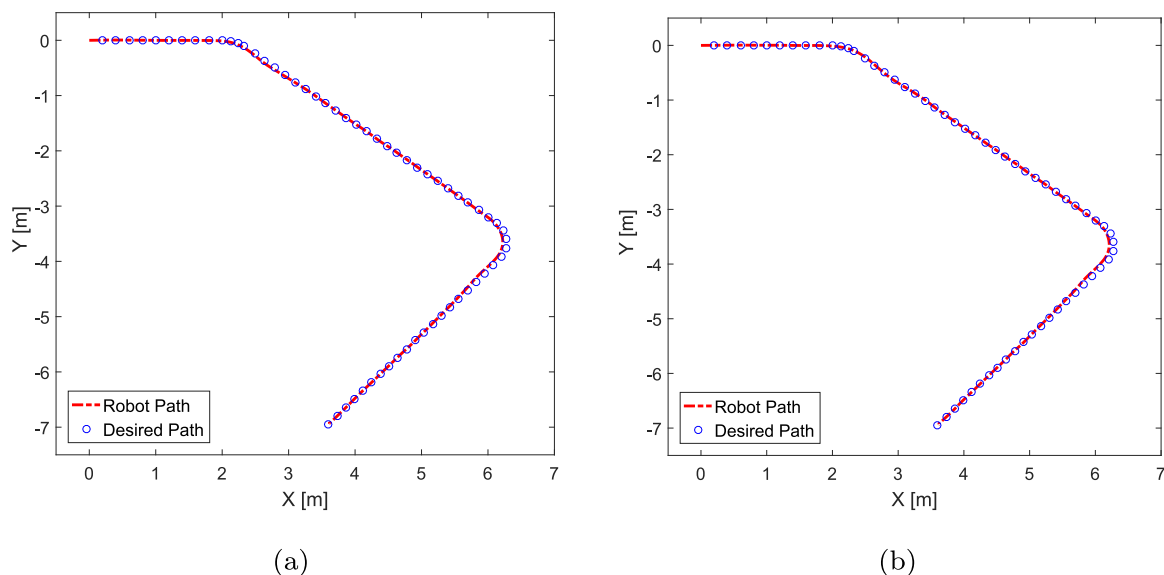
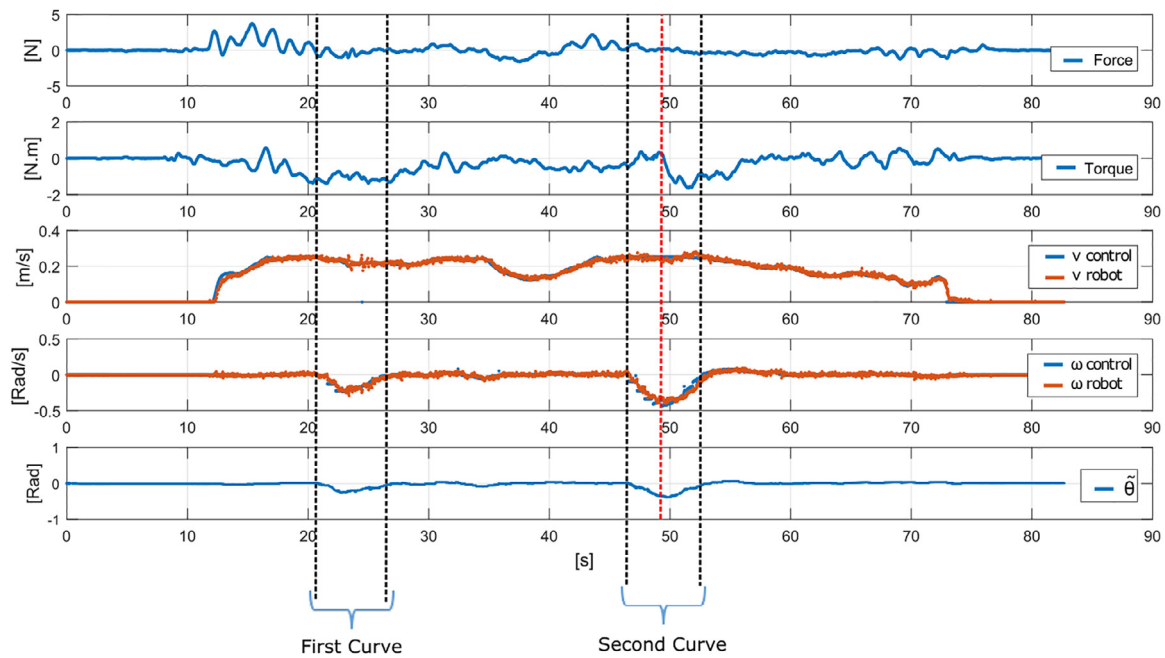
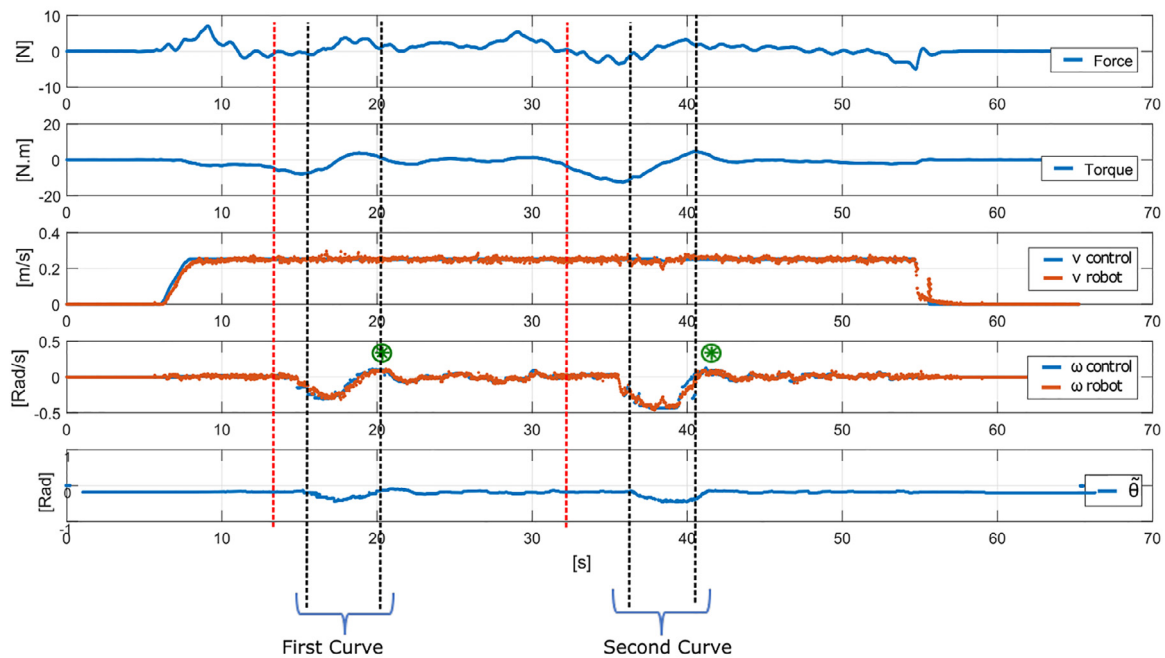


**Fig. 6.** Following the desired path. a) User wearing the blindfold. b) User without the blindfold.



(a)



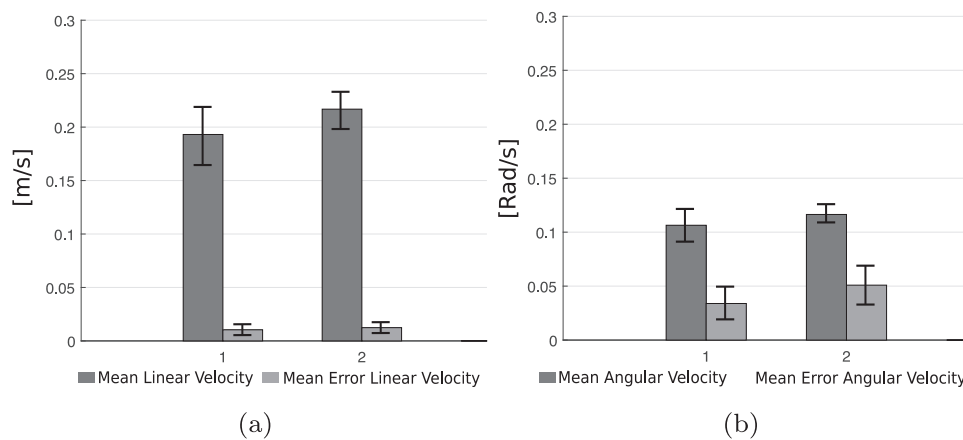
(b)

**Fig. 7.** a) Following the desired path using the blindfold. Up to down: user's force signal, user's torque signal, Control and SW linear velocities, Control and SW angular velocities,  $\theta$  signal. b) Following the desired path without use of blindfold. Up to down: user's force signal, user's torque signal, Control and SW linear velocities, Control and SW angular velocities,  $\theta$  signal.

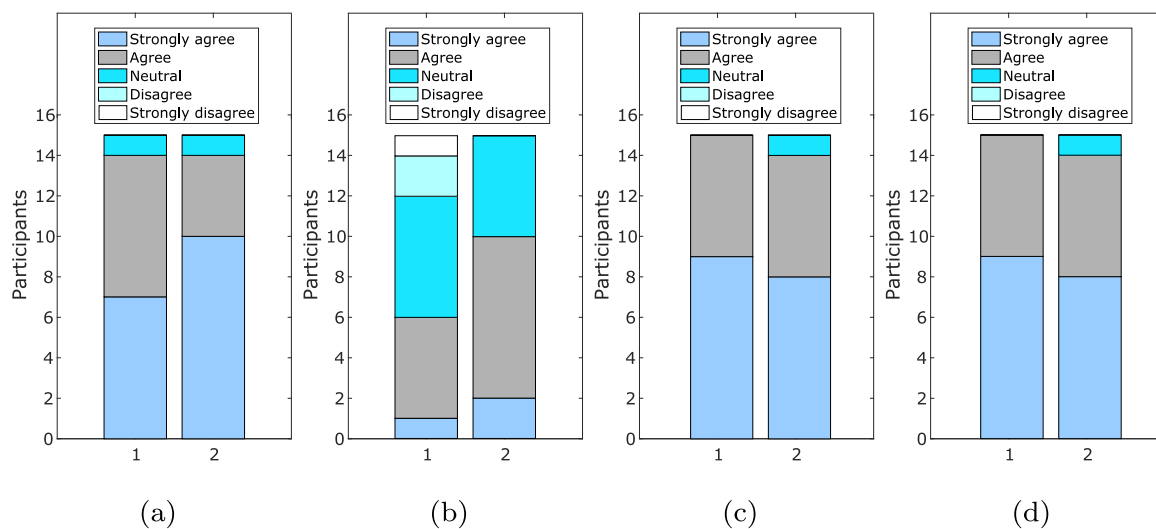
The mean linear velocity is 0.14 m/s, and the angular velocity only appears on the SW during the curves (maximum absolute value of 0.43 Rad/s). The orientation position error is approximately zero, because the guidance controller strategy keeps the user on the desired path (see Fig. 7a).

Fig. 7 b shows a representative result of the second part of the trials, performed without the blindfold. In this case, the visual feedback influences on user behavior, affecting force and torque

signals, which assumed larger values than previously. Thus, the user was more confident and felt that he/she had the control over the SW maneuverability (see Fig. 9b). In the straight line, the mean force value was of 1.5 N, with a maximum value of 5.4 N, and the human torque applied by the user is around 0 N.m. It can be observed that the user applied torque signal before the beginning of the second curve (see the red dotted line in Fig. 7b), which happened because the user could see the environment by where



**Fig. 8.** Group 1: Average data from all runs of the first part of the experiment, using the blindfold. Group 2: Average data from all participants without the use of the blindfold. (a) Statistic of linear velocity. (b) Statistic of the angular velocity.



**Fig. 9.** Qualitative evaluation for the guided experiments. Questions: a) 'I felt safe handling the SW'. b) 'I felt that I controlled the SW'. c) 'I felt that the SW was guiding me'. d) 'felt an intuitive interaction with the SW'. Column 1. Following the desired path using the blindfold. Column 2. Following the desired path without use of blindfold.

he/she was moving without being fully aware of the desired path to follow. Even though the user applied  $\tau_H(t)$ , the SW only took the turn direction when the curve began on the desired path. The absolute maximum torque value applied by the user was 12.6 N.m.

As the subject shown in Figure 7b felt safer in this experiment (see Fig. 9a), the linear velocity was always the maximum limited value, which was 0.25 m/s. This same behavior was observed on the signals obtained from 10 participants. In this case, the maximum absolute value of the angular velocity was 0.48 Rad/s, as the user applied  $\tau_H(t)$  because of the visual information. Furthermore, such visual feedback increments the user's perception of control. In other words, when perceiving the environment, users can better transmit their intentions to the SW, thus affecting the interaction torque and generating additional movement during the turns (see green asterisks in Fig. 7b). Nevertheless, the controller is capable of maintaining the SW on the desired path. Also, the orientation position error was also approximately zero. Both parts of the experiment, all participants followed the desired path using the haptic feedback of the control strategy (see Fig. 9c), which according to the perception of participants allowed an intuitive interaction between the user and the SW (see Fig. 9d).

Figure 8 a and b shows the mean velocities obtained by the users in the experiments, and the respective errors. It can be seen that the mean velocities tend to increase when the users does not

wear the blindfold. Additional to the mean and the standard deviation, a Mann-Whitney-Wilcoxon (MWW) tests were applied to the SW velocities. For both velocities, was used a significant level of 0.05 and a two-tailed hypothesis. Considering the linear velocity, its mean and standard deviation values change from  $0.1931 \pm 0.027$  m/s to  $0.2168 \pm 0.019$  m/s, with  $p$ -value of 0.023. The angular velocity also remains similar, passing from  $0.1064 \pm 0.014$  Rad/s to  $0.1164 \pm 0.009$  Rad/s, with  $p$ -value of 0.012. The  $p$ -values indicate that when the user is not using the blindfold, he/she really increment his/her gait speed. We believe that this is due to the fact that the users, who present no visual impairment, feel more comfortable and confident when not wearing the blindfold, leading to an increase on their gait speed. The mean error in the linear velocity is similar for both cases. In the case of the mean error in the angular velocity, the error is higher in the second part of the experiment, due to the SW arrived at the curve with a linear velocity higher and, according to the controller strategy, the angular velocity is directly proportional to the linear velocity.

In addition, from Figure 9 no significant differences were encountered between the two experiments. In order to analyze the Likert data, the MWW test was applied, as such test has a better response than  $t$ -test for small sample size [25]. Despite the MWW test has the equivalent power whit the  $t$ -test for Likert scales, the MWW test has a minimal type I error rates [26]. Using a significant

level of 0.05 and two-tailed hypothesis, the  $p$ -value obtained was 0.65272. This  $p$ -value does not reject the null hypothesis, which indicates, that the control strategy has a similar behavior when is using the blindfold and when is not. Likewise, this also indicates that the control strategy can be used to guide people with and without vision impairments, as in both conditions, the user understood the interaction way with the SW.

During the experiments, though many of the users reached the maximum linear velocity, no one commented on such limitation, which seems to be perceived as merely due the natural inertia of the SW. Users, in general, talked about the limiting speed value as a “good velocity for locomotion”. Moreover, they reported the perception of safety during guidance, and the interaction itself was considered intuitive along the desired path. In this sense, the control strategy does not require from the user a higher effort to maneuver the SW, allowing for guiding people through a desired path in a natural way.

## 5. Conclusions and future work

This paper presents a proposal for HREI to guide blind people with gait disorders. The haptic feedback given by the physical contact between the user and the SW generating guidance without the use of wearable devices. With the haptic feedback, an intuitive information about the path to be followed is provided, and the user is easily able to manage the use of the SW.

The control strategy proposed here allows for a comfortable user experience. The mass and damping parameters of the admittance controller did not demand higher effort by the user, and hence, the SW could be easily manipulated. By limiting the velocities of the SW and choosing a coherent path design, the control strategy behaved properly and transmitted comfort and safety to the user.

As future work, new control strategies are being developed to promote the haptic feedback for the user of the SWs, and as a consequence, improve the HREI. With the RP-LIDAR sensor, the aim is to improve the perception of the environment and, through probabilistic techniques, such as SLAM, to generate, in real time, adequate paths that the SW should follow to avoid obstacles and reach a specific location. In addition, it is necessary to evaluate the interaction parameters to improve the HREI. We believe that this field of research provides real life advances towards the assistance in the mobility of visually impaired people. The clinical validation will be the focus of the next paper. During the tests to validate the guiding strategy, the special interest will be on the guidance, learning and vision effect. The idea is to do a crossover design of the test, varying the path and the number of test sessions over time to highlight the aforementioned effects.

## Declaration of Competing Interest

None declared.

## Ethical Approval

Federal University of Espírito Santo, UFES/Brazil. Protocol number - CAEE: 64797816.7.0000.5542

## Acknowledgements

This research is supported by CAPES (grant number 88887.095626 / 2015-01), FAPES (grant number 80709036) and CNPq (grant number 304192 / 2016-3). The research leading to these results also received funding from the European Commission H2020 program under grant agreement no. 688941 (FUTEBOL), as well from the Brazilian Ministry of Science, Technology, Innovation, and Communication (MCTIC) through RNP and CTIC.

## Supplementary material

Supplementary material associated with this article can be found, in the online version, at doi:[10.1016/j.medengphy.2020.04.002](https://doi.org/10.1016/j.medengphy.2020.04.002).

## References

- [1] World Health Organization. Universal eye health. A global action plan 2014–2019. Tech. Rep.; 2014.
- [2] United Nations, Department of Economic and Social Affairs Population Division. World Population Ageing 2017 - Highlights; 2017. ISBN 9789211515510. [http://www.un.org/en/development/desa/population/publications/pdf/ageing/WPA2017\\_Highlights.pdf](http://www.un.org/en/development/desa/population/publications/pdf/ageing/WPA2017_Highlights.pdf)
- [3] Pirker W, Katzenschlager R. Gait disorders in adults and the elderly: a clinical guide. Wien Klin Wochenschr 2017;129(3–4):81–95. doi:[10.1007/s00508-016-1096-4](https://doi.org/10.1007/s00508-016-1096-4).
- [4] Alexander NB, Goldberg A. Gait disorders: search for multiple causes. Cleve Clin J Med 2005;72(7):586–600.
- [5] Crews JE, ACampbell V. Vision impairment and hearing loss among community dwelling older americans: implications for health and functioning. Am J Public Health 2004;94(5):823–829.
- [6] Deshen S, Deshen H. On social aspects of the usage of guidedogs and long-canes. Sociol Rev 1989;37(1):89–103. doi:[10.1111/j.1467-954X.1989.tb00022.x](https://doi.org/10.1111/j.1467-954X.1989.tb00022.x).
- [7] Wachaja A, Agarwal P, Zink M, Adame MR, Möller K, Burgard W. Navigating blind people with walking impairments using a smart walker. Auton Robots 2016;2015–Decem:1–19. doi:[10.1007/s10514-016-9595-8](https://doi.org/10.1007/s10514-016-9595-8).
- [8] Bradley SM, Hernandez CR. Geriatric assistive devices. Am Fam Physician 2011;84(4):405–11.
- [9] Martins MM, Santos CP, Frizera-Neto A, Ceres R. Assistive mobility devices focusing on smart walkers: classification and review. Rob Auton Syst 2011;60(4):548–62. doi:[10.1016/j.robot.2011.11.015](https://doi.org/10.1016/j.robot.2011.11.015).
- [10] Jiménez MF, Monllor M, Frizera A, Bastos T, Roberti F, Carelli R. Admittance controller with spatial modulation for assisted locomotion using a smart walker. J Intell Robot Syst 2018;1–17. doi:[10.1007/s10846-018-0854-0](https://doi.org/10.1007/s10846-018-0854-0).
- [11] Spenko M, Yu H, Dubowsky S. Robotic personal aids for mobility and monitoring for the elderly. IEEE Trans Neural Syst Rehabil Eng 2006;14(3):344–51.
- [12] Bousbia-Salah M, Bettayeb M, Larbi A. A navigation aid for blind people. J Intell Robot Syst 2011;64(3–4):387–400. doi:[10.1007/s10846-011-9555-7](https://doi.org/10.1007/s10846-011-9555-7).
- [13] Geravand M, Werner C, Hauer K, Peer A. An integrated decision making approach for adaptive shared control of mobility assistance robots. Int J Soc Robot 2016;8(5):631–48. doi:[10.1007/s12369-016-0353-z](https://doi.org/10.1007/s12369-016-0353-z).
- [14] Andò B, Graziani S. Multisensor strategies to assist blind people: a clear-path indicator. IEEE Trans Instrum Meas 2009;58(8):2488–94. doi:[10.1109/TIM.2009.2014616](https://doi.org/10.1109/TIM.2009.2014616).
- [15] Pons (CSIC) JL. Wearable robots: biomechatronic exoskeletons. Madrid: John Wiley & Sons Ltd; 2008.
- [16] Werner C, Ullrich P, Geravand M, Peer A, Bauer JM, Hauer K. A systematic review of study results reported for the evaluation of robotic rollators from the perspective of users. Disabil Rehabil 2017;0(0):1–12. doi:[10.1080/17483107.2016.1278470](https://doi.org/10.1080/17483107.2016.1278470).
- [17] Lin Q, Han Y. A context-aware-based audio guidance system for blind people using a multimodal profile model. Sensors (Switzerland) 2014;14(10):18670–700. doi:[10.3390/s141018670](https://doi.org/10.3390/s141018670).
- [18] Motta G, et al. Mobility of visually impaired people: fundamentals and ICT assistive technologies. Cham: Springer; 2018. doi:[10.1007/978-3-319-54446-5\\_16](https://doi.org/10.1007/978-3-319-54446-5_16).
- [19] Lacey G. Context-Aware shared control of a robot mobility aid for the elderly blind. Int J Rob Res 2000;19(11):1054–65. doi:[10.1177/02783640022067968](https://doi.org/10.1177/02783640022067968).
- [20] Lacey GJ, Rodriguez-Iosada D. The evolution of guido. IEEE Robot Autom Mag 2008;15(December):75–83. doi:[10.1109/MRA.2008.929924](https://doi.org/10.1109/MRA.2008.929924).
- [21] Lu CK, Huang YC, Lee CJ. Adaptive guidance system design for the assistive robotic walker. Neurocomputing 2015;170:152–60. doi:[10.1016/j.neucom.2015.03.091](https://doi.org/10.1016/j.neucom.2015.03.091).
- [22] Cifuentes CA, Frizera A. Human-Robot interaction strategies for locomotion. Springer International Publishing Switzerland; 2016. doi:[10.1007/978-3-319-34063-0](https://doi.org/10.1007/978-3-319-34063-0).
- [23] Andaluz VH, Roberti F, Toibero JM, Carelli R, Wagner B. Adaptive dynamic path following control of an unicycle like mobile robot. In: Intelligent robotics and applications; chap. 56. Springer Berlin Heidelberg; 2011. p. 563–74. doi:[10.1007/978-3-642-25486-4\\_56](https://doi.org/10.1007/978-3-642-25486-4_56).
- [24] Peel NM, Kuys SS, Klein K. Gait speed as a measure in geriatric assessment in clinical settings: a systematic review. J Gerontol 2012;68(1):39–46. doi:[10.1093/gerona/gls174](https://doi.org/10.1093/gerona/gls174).
- [25] Clifford R. A Comparison of the Power of Wilcoxon's Rank-Sum Statistic to That of Student's t Statistic under Various Nonnormal Distributions Author (s): R. Clifford Blair and James J. Higgins Published by : American Educational Research Association and Ameri. Journal of Educational Statistics 1980;5(4):309–35. doi:[10.2307/1164905](https://doi.org/10.2307/1164905). <http://www.jstor.org/stable/1164905>
- [26] de Winter JC, Dodou D. Five-point likert items: t test versus Mann-Whitney-Wilcoxon. Pract Assess Res Eval 2010;15(11).